FULL PAPERS

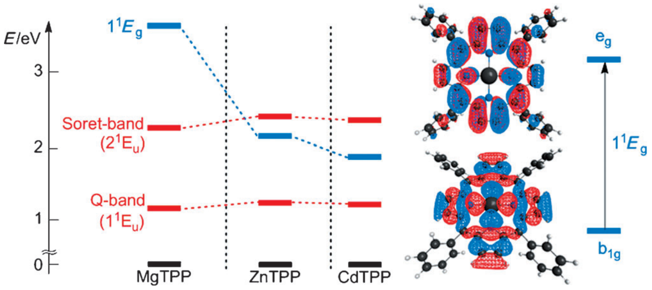

Stab in the dark: By means of transient absorption studies, following Q- and Soret-band excitation, and ab initio calculations on *meso*-tetraphenylporphyrinato magnesium(II) (MgTPP) and *meso*-tetraphenylporphyrinato cadmium(II) (CdTPP), it is shown that electronic relaxation following Soret-band excitation of porphyrins with a heavy central atom is mediated by a hitherto disregarded dark state (see picture).

*Y. Liang, M. Bradler, M. Klinger, O. Schalk, M. C. Balaban, T. S. Balaban, E. Riedle, A.-N. Unterreiner**

■■ – ■■

Ultrafast Dynamics of *meso*-Tetraphenylmetalloporphyrins: The Role of Dark States

DOI: 10.1002/cplu.201300143

Ultrafast Dynamics of *meso*-Tetraphenylmetalloporphyrins: The Role of Dark States

Yu Liang,[a] Maximilian Bradler,[b] Melanie Klinger,[a] Oliver Schalk,[b, c] Mihaela Carmen Balaban,[d, e] Teodor Silviu Balaban,[d, e] Eberhard Riedle,[b] and Andreas-Neil Unterreiner*[a]

Studying the relaxation pathways of porphyrins and related structures upon light absorption is crucial to understand the fundamental processes of light harvesting in biosystems and many applications. Herein, we show by means of transient absorption studies, following Q- and Soret-band excitation, and ab initio calculations on *meso*-tetraphenylporphyrinato magnesium(II) (MgTPP) and *meso*-tetraphenylporphyrinato cadmium(II) (CdTPP) that electronic relaxation following Soret-band excitation of porphyrins with a heavy central atom is mediated by a hitherto disregarded dark state. This accounts for an increased rate of internal conversion. The dark state originates from an orbital localized at the central nitrogen atoms and its energy continuously decreases along the series from magnesium to zinc to cadmium to below 2.75 eV for CdTPP dissolved in tetrahydrofuran. Furthermore, we are able to directly trace fast intersystem crossing in the cadmium derivative, which takes place within (110±20) ps.

Introduction

Cyclic tetrapyrroles and their derivatives are ubiquitous natural pigments and play an important role in nature. For example, hemoglobin in heme proteins is responsible for oxygen transport in blood, whereas chlorophyll in plant cells is part of the light-harvesting system that regulates photosynthesis. Its functionality can be tuned by several factors, such as the C–N skeleton, which can be saturated to a certain degree; the surroundings, for example, a protein environment; and the central metal atom. In recent years, porphyrin derivatives were investigated for different purposes, such as light-harvesting complexes in solar cells,[1] photodynamic therapy in medicine,[2] and electronic devices.[3] Consequently, there is much interest in the optical properties and photophysical behavior of porphyrins.[4–7] To better understand these properties, model systems such as metal *meso*-tetraphenylporphyrins (MTPP, M = Mg, Cd) were chosen for investigation.[8]

A simplified molecular structure is presented in Figure 1. Its symmetry is supposed to be close to D_{4h}. However, in the minimum energy geometry, the four peripheral phenyl rings are known to be twisted by 65–70° with respect to the porphyrin skeleton;[10–13] this lowers the symmetry to C_{2v}. In coordinating solvents, magnesium atoms in chlorophylls or porphyrins become five- or even sixfold coordinated, which reduces the symmetry further. The electronic structure of porphyrins in the free-base or metal-coordinated forms is largely characterized by their absorption and fluorescence spectra.[14–18] For metals with closed d shells, the absorption spectra consist of an intense band at $\lambda \approx 420$ nm in the blue/ultraviolet spectral region (characteristic of the Soret band, also called the B band) with a blueshifted shoulder assigned to another close-lying

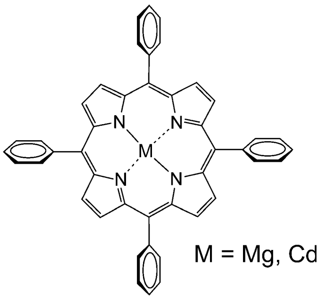

Figure 1. Molecular structure of *meso*-tetraphenylporphyrinato metal(II) complexes. In addition to the four-fold coordinated species implied, M·THF and THF·M·THF can also be present.[9]

---

[a] Dr. Y. Liang, Dr. M. Klinger, Dr. A.-N. Unterreiner
Institute for Physical Chemistry and Center for Functional Nanostructures
Karlsruhe Institute of Technology (KIT)
Fritz-Haber-Weg 2, 76131 Karlsruhe (Germany)
E-mail: andreas.unterreiner@kit.edu

[b] M. Bradler, Dr. O. Schalk, Prof. Dr. E. Riedle
Lehrstuhl für BioMolekulare Optik
Ludwig-Maximilians-Universität
Oettingenstraße 67, 80538 München (Germany)

[c] Dr. O. Schalk
Stockholm University, AlbaNova University Center
Roslagstullsbacken 21, 106 91 Stockholm (Sweden)

[d] M. C. Balaban, Prof. Dr. T. S. Balaban
Institute for Nanotechnology and Center for Functional Nanostructures
Karlsruhe Institute of Technology (KIT) (Germany)

[e] M. C. Balaban, Prof. Dr. T. S. Balaban
Present address:
Aix Marseille Université, CNRS, iSm2 UMR 7313
13397 Marseille (France)

Supporting information for this article is available on the WWW under http://dx.doi.org/10.1002/cplu.201300143.

state.[19] Two weaker absorption maxima in the visible region between $\lambda = 550$ and 650 nm are assigned to the Q bands. The next higher-lying state in MgTPP is at $\lambda \approx 360$ nm. The fifth and more prominent absorption band lies at $\lambda \approx 320$ nm and is called the N band.[20] All of these bands have E_u symmetry and are assigned to $\pi\pi^*$ transitions. These can be qualitatively explained by means of the well-established Gouterman four-orbital model[21–23] or, more convincingly, by the molecular orbital (MO) interpretation of Baerends et al.[24] In the context of this paper, this interpretation is sufficient. However, higher states are better described by more advanced models, for example, those from Solheim et al.[25] or Peralta et al.[26] In the MO interpretation, the electronic structure is explained by the interaction of the four pyrrole rings ($(Py)_4^{2-}$ cage) with CH methine bridges. For a metalloporphyrin, this leads to several e_g orbitals and non-degenerate ungerade states. The Q and Soret bands arise from excitation between the two highest occupied orbitals, which have a_{1u} and a_{2u} symmetry and a pair of e_g orbitals (LUMO). The higher $\pi\pi^*$ transitions in the UV region are mainly from lower lying ungerade states to the LUMO. The fluorescence spectrum exhibits a small Stokes shift. In addition to emission from the Q band, one also observes fluorescence from the Soret band.[27,28]

Photophysical properties of many diamagnetic metalloporphyrin derivatives, such as ZnTPP, MgTPP and CdTPP (TPP = tetraphenylporphyrinato), have been studied after excitation to the Soret band. Fluorescence up-conversion experiments of Zewail and co-workers showed that, for ZnTPP in benzene, the fluorescence lifetime of the Soret band was measurably longer than the rise time of the Q-band fluorescence and was interpreted by the presence of an additional state close to the Soret band.[29] These findings could not be confirmed by other groups;[28,30–34] however, a small fraction of excited ZnTPP molecules was found to bypass the Q band.[4,35] In MgTPP, the efficiency of S_2–S_1 relaxation was close to unity, whereas it is decreased to 70% in CdTPP.[30] As possible explanations for this behavior, reaction paths through dark gerade states and the triplet-manifold[30–33,35–37] were proposed. Evidence for the existence of dark states has been given by time-dependent (TD) DFT calculations[38–41] and by direct access upon Q-band excitation and near-infrared (NIR) probe in tetratolyl derivatives (*meso*-tetra-*para*-tolyl-*21H,23H*-porphyrin ($TTP-H_2$) and ZnTTP).[42] Most recently, Hopkins and co-workers examined the transient absorption spectra of ZnTPP in the NIR region.[43] They assigned the NIR bands to transitions from the Q band to gerade-symmetry dark states. The role these states might play in the relaxation pathway of (metallo)porphyrins upon Soret excitation necessitates additional information about their origin, for example, from a complete set of experimental data in the series 2H, Mg, Zn, Cd. Hence, we studied transient absorption of MgTPP and CdTPP dissolved in tetrahydrofuran (THF) upon excitation to the Q and the Soret band and scanned the probe wavelength with various white lights covering the region between $\lambda = 290$ and 1660 nm. These experiments allowed dark states to be located up to the N band and also a comparison of transient spectra upon Q and Soret band excitation; thus it is possible to decipher pathways the molecule may take upon Soret excitation. Additionally, TDDFT calculations were performed on several TPP derivatives. Based upon experimental findings and calculations, a model for the relaxation pathway of these molecules upon Soret excitation is presented and sheds light on apparent inconsistencies presented in the literature to date.

Results and Discussion

Steady-state absorption and emission spectra

Steady-state absorption and emission spectra of MgTPP and CdTPP in THF are shown in Figure 2. In the absorption spectrum, the maxima of the Soret bands ($2E_u$ symmetry) were found at $\lambda = 429$ nm (2.89 eV) for MgTPP and $\lambda = 431$ nm (2.87 eV) for CdTPP with a small shoulder on their blue sides at $\lambda = 409$ nm (3.03 eV) for MgTPP and $\lambda = 411$ nm (3.02 eV) for CdTPP. These shoulders are assigned to the higher lying $3E_u$ state. The peaks of the Q band ($1E_u$ symmetry) were observed at $\lambda = 613$ (610) nm for the Q(0,0) band and $\lambda = 571$ (569) nm for the Q(1,0) band, along with a smaller shoulder at 530 (529) nm for MgTPP (CdTPP). The Q-band absorptions can be understood in terms of vibrational progressions with an energy splitting of about 1170 cm^{-1}.[44] The $S_1 \rightarrow S_0$ emission spectra of both porphyrins are mirror images of the corresponding absorption spectrum. The emission band originating from the first excited state Q(0,0) has a maximum at $\lambda = 617$ nm for MgTPP and $\lambda = 626$ nm for CdTPP. The second, weaker band corresponding to the Q(1,0) transition was observed at $\lambda = 671$ nm for MgTPP and $\lambda = 665$ nm for CdTPP. The emission spectra show Stokes shifts of roughly 120 cm^{-1} for MgTPP and 434 cm^{-1} for CdTPP. The fluorescence yield of CdTPP is much lower than that of MgTPP; this was attributed to fast intersystem crossing (ISC) in CdTPP in previous experiments.[45]

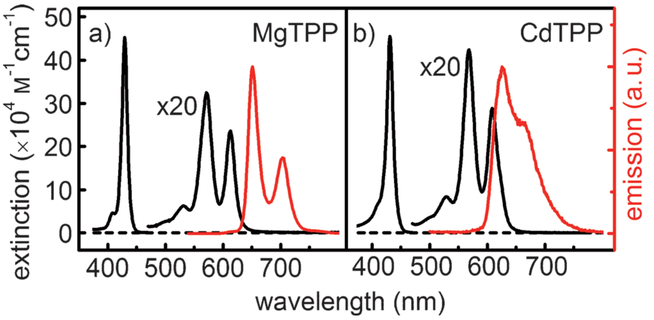

Figure 2. Steady-state absorption and emission spectra of (a) MgTPP and (b) CdTPP in THF at room temperature; emission spectra were excited at $\lambda = 431$ nm for CdTPP and $\lambda = 429$ nm for MgTPP.

TDDFT calculations

To study the absorption spectrum of the one-color forbidden gerade states, we performed TDDFT calculations on MgTPP and CdTPP using the GAMESS package[46,47] and compared

Table 1. Electronic energy levels [eV] of MgTPP, ZnTPP, CdTPP, and TPP-H_2, as calculated with different DFT functionals in the 6-31G* basis set. Geometries were calculated at the B3LYP/6-31G* level with C_{2v} symmetry.

	MgTPP				ZnTPP				CdTPP				TPP-H_2			
	B3LYP	BP86	M05-2X	OPBE	B3LYP	BP86	M05-2X	OPBE	B3LYP	BP86	M05-2X	OPBE	B3LYP	BP86	M05-2X	OPBE
Q state	2.232	2.1	2.299	2.112	2.293	2.14	2.364	2.155	2.278	2.082	2.4	2.116	2.136	2.081	2.17	2.034
	–	–	–	–	–	–	–	–	–	–	–	–	2.281	2.136	2.381	2.153
B state	3.225	3.018	3.416	3.04	3.337	3.055	3.456	3.078	3.312	3.07	3.493	3.095	3.146	3.095	3.382	3.121
	–	–	–	–	–	–	–	–	–	–	–	–	3.265	3.133	3.462	3.158
3^1E_u state	3.625	3.08	4.28	3.116	3.688	3.151	4.225	3.18	3.668	3.134	4.36	3.163	–	–	–	–
3^1B_{2u} state	–	–	–	–	–	–	–	–	–	–	–	–	3.553	2.855	4.111	2.872
3^1B_{3u} state	–	–	–	–	–	–	–	–	–	–	–	–	3.563	2.898	4.395	2.913
1 “$e_g \otimes e_g$”	3.617	3.122	4.198	3.146	3.61	3.112	4.194	3.139	3.533	3.047	4.133	3.076	3.74	3.126	4.665	3.154
2 “$e_g \otimes e_g$”	3.666	3.13	4.249	3.129	3.656	3.142	4.261	3.169	3.576	3.07	4.202	3.099	3.867	3.255	4.537	3.264
$d_{x^2-y^2}$ state	4.471	4.452	4.489	4.447	3.169	2.398	–	2.492	2.969	2.332	3.86	2.4	3.306	2.842	3.849	2.853
	–	–	–	–	–	–	–	–	–	–	–	–	3.475	2.879	4.307	2.889

them with ZnTPP, TPP-H_2, and MgP (magnesium porphyrin without any substituents).[24,38] Ground-state geometries were calculated at the B3LYP/6-31G* level under the restriction of both D_{4h} and C_{2v} symmetry. Symmetry labels are given based on D_{4h} (D_{2d} in the case of TPP-H_2) in agreement with Solheim et al.[25] Singlet excitation energies for C_{2v} symmetry were calculated at the B3LYP/6-31G* level and compared with various functionals (BP86, OPBE, and M05-2X) using the same basis set. B3LYP results and a comparison of the different methods are shown in Table 1, and geometries are given in the Supporting Information.

There is a long history of interpreting the excited states of porphyrins (see the Introduction). Herein, we use the MO interpretation of Baerends et al.[24] to address a few points: Comparing MgP and MgTPP, one important feature is the energetic difference between equivalent states (about 0.15–0.3 eV). The phenyl group at the methine bridge of MgTPP allows slightly better stabilization than the C–H bond of MgP, which is governed partly by the hyperconjugation effect caused by tilting of the phenyl group; thus reducing the interaction between the bridges and the $(Py)_4^{2-}$ cage. This lowers the $5e_g$ state and raises the $4e_g$ state. As a consequence, the gap between the (nearly) unaffected $4a_{2u}$ and $1a_{1u}$ states (HOMO and HOMO−1, the orbital numbering is adopted from MgP) and the $5e_g$ state (LUMO) decreases, leading to a redshift in the absorption spectrum. The differences in the theoretical values for the Q and Soret band ($1E_u$ and $2E_u$) between MgP and MgTPP of 0.16 and 0.28 V, respectively, are in good agreement with the experimental values of 0.11 and 0.23 eV, respectively (see Ref. [48] for a discussion of the spectrum of MgP). The excited states of the TPP derivatives investigated are not very sensitive with respect to the central metal ion (Mg, Zn, and Cd): they all have no open d shells, the same charge, and similar radii, although Cd^{2+} is about 20 pm larger[49] and even small changes in the radius might lead to serious distortions of the ring (see below). The excited-state manifold consists of a set of E_u states that represent the visible absorption spectrum and a variety of different gerade states. The E_u states of the B3LYP calculations are approximately 0.2 eV higher in energy than the experimental values, but seem to be better represented by both the BP86 and OPBE-functionals (see Ref. [50] for cold gas-phase spectra of ZnTPP and TPP-H_2 in He). The description of the gerade states turns out to be more challenging. These consist of 4 states, following an $e_g \rightarrow e_g$ excitation between 3.6 and 3.9 eV (B3LYP) that cannot be assigned to a certain symmetry, because $e_g \otimes e_g = a_{1g} \otimes a_{2g} \otimes b_{1g} \otimes b_{2g}$ (a_1 and a_2 have C_{2v} symmetry) and a B_{2g} state following HOMO to LUMO+1 excitation at around 4.0 eV. The $e_g \rightarrow e_g$ states are significantly reduced by 0.5 eV in energy when using BP86 and OPBE, which brings them close to the Soret excitation. The crucial difference between the molecules with different central metal atoms, however, is an E_g state that results from excitation from a b_{1g} orbital to the LUMO. This orbital is localized at the central nitrogen atoms of the porphyrin skeleton and interacts with an unoccupied $d_{x^2-y^2}$ orbital at the central metal (see Figure S1 in the Supporting Information). In MgTPP, the d manifolds are empty and at B3LYP/6-31G* level the state is located at 4.46 eV, which is on the blue side of the Soret band. In ZnTPP, however, the orbital becomes significantly destabilized owing to interaction of the larger $4d_{x^2-y^2}$ orbital, compared with the $3d_{x^2-y^2}$ orbital in MgTPP, which causes poorer overlap with the N cage. This lowers the gap to the LUMO and reduces the excitation energy to 3.17 eV, which places this state between the Q and Soret bands. This effect is even more pronounced in CdTPP, in which the excitation energy drops to 2.96 eV concomitantly with an increase in the ion radius (see Table 1). The energy of the state significantly varies with the functional. For BP86 and OPBE, it is placed only 0.3–0.35 eV above the Q band for CdTPP and ZnTPP. A comparison of these results with experimental results and a comment on the applicability of DFT for calculations of this type is given in the next section. The most significant difference between the metalated porphyrins and TPP-H_2 is the reduction of the symmetry to D_{2h}. This reduction leads to a splitting not only of the Q band (Q_x and Q_y), but also of the E_g transition centered at the nitrogen atoms. The latter state turns into B_{1g} and A_g states, which are separated by 0.2 eV.

Transients of MgTPP

To discuss the role of the dark states and the existence of the "unknown channel" in CdTPP, we first address the features of

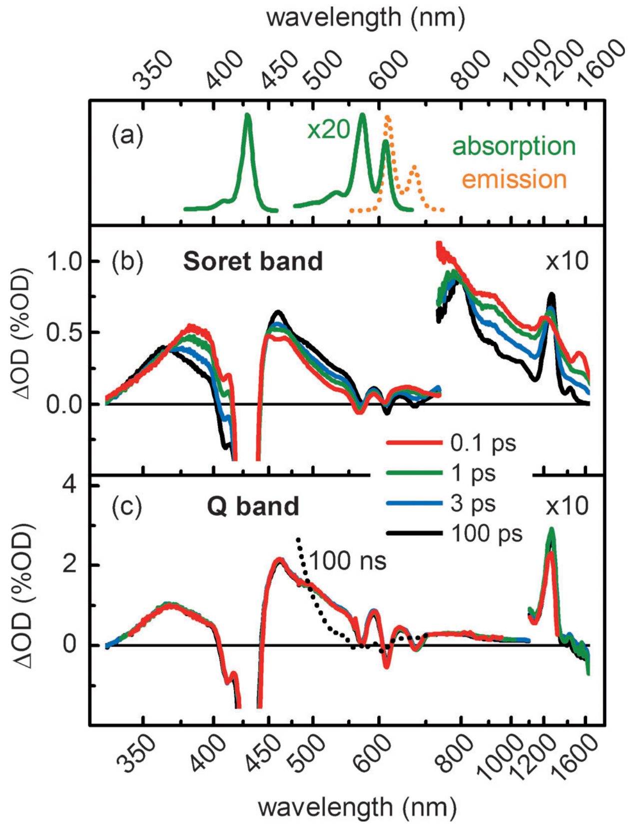

Figure 3. a) Absorption and emission spectra of MgTPP, (b) transient spectra after excitation of the Soret band at $\lambda = 425$ nm, and (c) transient spectra after excitation of the Q band at $\lambda = 620$ nm. For clarity, the early time spectra in (c) are clipped in the display to indicate that all four show spectra are identical within experimental precision.

the transient spectra of MgTPP, which act as a reference, but are interesting in themselves. Transient spectra at delay times of 0.1, 1, 3, and 100 ps, ranging between $\lambda = 320$ and 1700 nm, are shown in Figure 3 for excitation to the Soret band at $\lambda = 425$ nm (Figure 3 b) and excitation to the Q band at $\lambda = 620$ nm (Figure 3 c). The data can be fitted with a global fitting routine to a sum of exponential functions, as given by Equation (1):

$$S_i(t,\lambda) = \sum{}_i a_i(\lambda)\exp\left(-\frac{t}{\tau_i}\right) \otimes g(t,\lambda) \qquad (1)$$

in which τ_i are the exponential decay constants, $a_i(\lambda)$ are the decay-associated difference spectra (DADS), and $g(t,\lambda)$ is the experimental response function, including the chirp (see Ref. [51]). The DADS for MgTPP are shown in Figure 4 and consist of three (four) components for Q-band (Soret-band) excitation. The spectra predominantly exhibit excited-state absorption (ESA) with contributions from ground-state bleaching (GSB) in the Soret- and Q-band regions and stimulated emission (SE) in the region between $\lambda = 600$ and 700 nm. Upon Soret excitation, the appearance of the SE band is delayed by $\tau_1 = 3.2$ ps, so we can assign the first time constant to internal conversion from the Soret to the Q band, in agreement with previous reports.[30,35] The third component of 7 ns was obtained with our ns-setup, with which we only probed the visible region, and which can be assigned to ISC,[45] while recovery of the ground state takes place within more than 1 μs. For the last two time constants, the DADS are almost identical and signify that relaxation from the Soret to Q band upon excitation at $\lambda = 425$ nm takes place with (almost) unity quantum yield; this is in agreement with analysis from the Steer group.[30] The second time constant cannot unambiguously be assigned to an electronic relaxation and its amplitude is largest in the vicinity of strong modulations of the transient spectrum, that is, close to the regions where GSB and SE can be observed. This is an indication that we observe a shift of the bands which would represent a vibrational relaxation of the molecules. This can be confirmed when analyzing the shift of the band maxima. An exemplary shift of the Q(1,0) GSB for Q- and Soret-band excitation and details of the analysis is given in Figure S2 in the Supporting Information. These shifts confirm that cooling of porphyrins is a complex process, which takes place on at least two timescales (1–3 ps and >10 ps). Hence, the time constant obtained by the global fitting routine probably has no significant meaning. Accordingly, Brixner and co-workers[34] assigned a time interval ranging between 10 and 100 ps to vibrational relaxation of the Q band of ZnTPP in ethanol.

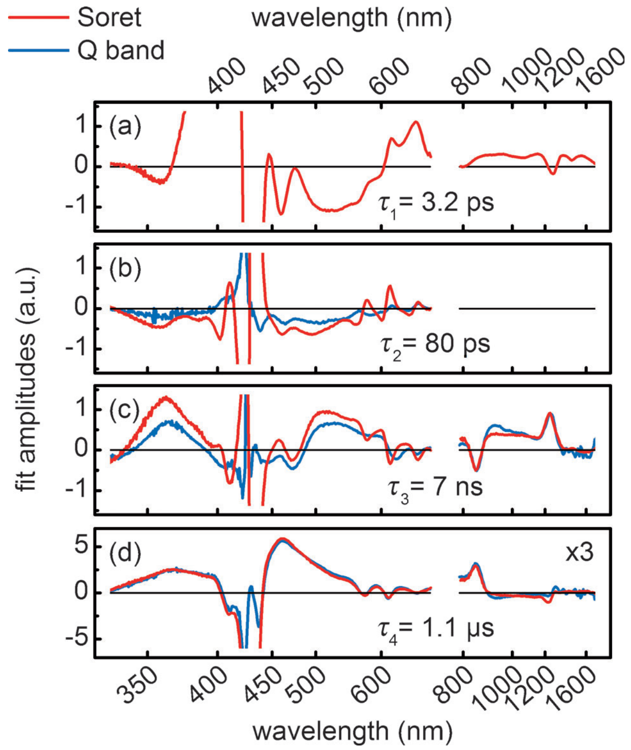

Figure 4. DADS for MgTPP upon excitation of the Q(0,0) (blue) and Soret (red) bands.

The spectral shape of the ESA signal is the test case to judge the dynamics of MgTPP. The dominant band in the IR (after relaxation to the Q band) region has a maximum at $\lambda \approx 1280$ nm (0.97 eV), and a minor maximum can be found at $\lambda \approx 1430$ nm (0.86 eV). When summing up the energies from the Q(0,0) band (2.02 eV) and the ESA maxima, one realizes that the total energy for the major peak is 2.99 eV, which is exactly the excitation energy of the $3E_u$ band, whereas the energy of the side peak (2.88 eV) corresponds to the energy of the Soret band (see also Figure S3). Because it is known that there are no dark gerade states below the Soret band in MgTPP (see the TDDFT calculations section), this essentially shows that the oscillator strength between the Q and Soret bands is significantly decreased with respect to the $3E_u$ band. On the other hand, ESA on the blue side of the $3E_u$ band is relatively structureless, which is in agreement with the UV/Vis spectrum that also has no marked maximum on the blue side of the Soret/$3E_u$ band. In conclusion, there is no evidence for ESA to a gerade state in the MgTPP data. The similarities of a strong ESA signal between $\lambda = 1250$ and 1300 nm in MgTPP, ZnTPP, and CdTPP furthermore show that these bands cannot be addressed to a dark state in the other porphyrins, in contrast to the analysis of Hopkins et al. who only considered zinc–porphyrins.[43] As a final result, according to the literature values,[52] we state that the triplet splitting (T_1 and T_3) in MgTPP is 1.44 eV ($\lambda = 860$ nm), as shown by the DADS in Figure 4 and the complete transient spectra in Figure S4 in the Supporting Information.

Transients of CdTPP

Transient spectra of CdTPP following excitation at $\lambda = 425$ (Soret band) and 620 nm (Q band) are shown in Figure 5 and their DADS are presented in Figure 6 together with the DADS from the data following excitation of the Q(1,0) band at $\lambda = 569$ nm. The spectra bear some resemblance to the spectra of MgTPP. The GSB and SE structure in the regions of the Soret- and the Q-band excitations show similar behavior and the ESA structures are alike. As expected, there are a few well-known deviations: Opposite to MgTPP, the Q band is reached within 230 fs upon Soret excitation and ISC proceeds within 120 ps instead of 7 ns, which is mainly caused by the strong spin-orbit coupling (heavy-atom effect)[45] of the central cadmium atom. These findings agree nicely with results in the literature.[30] In the following, we discuss 1) the dynamics upon Soret excitation and compare them with the findings in MgTPP and 2) the spectrum of the gerade states of CdTPP.

In a previous study, the energy gap law was taken as an indication that part of the population (30%) generated by Soret-band excitation was bypassing the Q band.[30] There are several alternative pathways available: 1) depopulation directly to the ground state, 2) ISC from the Soret band to the triplet manifold, and 3) internal conversion to the "dark" $1E_g$ state. However, inspection of the DADS for excitation to the Q and Soret bands reveals that the spectra are identical within two percent, in addition to the existence of the 230 fs component in the case of Soret excitation. Moreover, no spectral features appear in the transient spectrum between $\lambda = 290$ and 1660 nm, which could be caused by probing either the triplet state or the $1E_u$ state. In addition, the dynamics cannot be caused by direct repopulation of the ground state because this should be seen in the GSB spectrum at $\lambda = 569$ nm. Bleaching, however, does not seem to change significantly within the first few ps. Hence, the only remaining explanation of the spectra is quantitative (100 ± 2)% population of the Q band within 230 fs. Because direct internal conversion would be in disagreement with the energy gap law applied in the work of Steer and coworkers,[30] it is likely that internal conversion between the Soret and Q bands is mediated by a close-lying state. If this is the case, the only candidate would be the dark E_g state (see below).

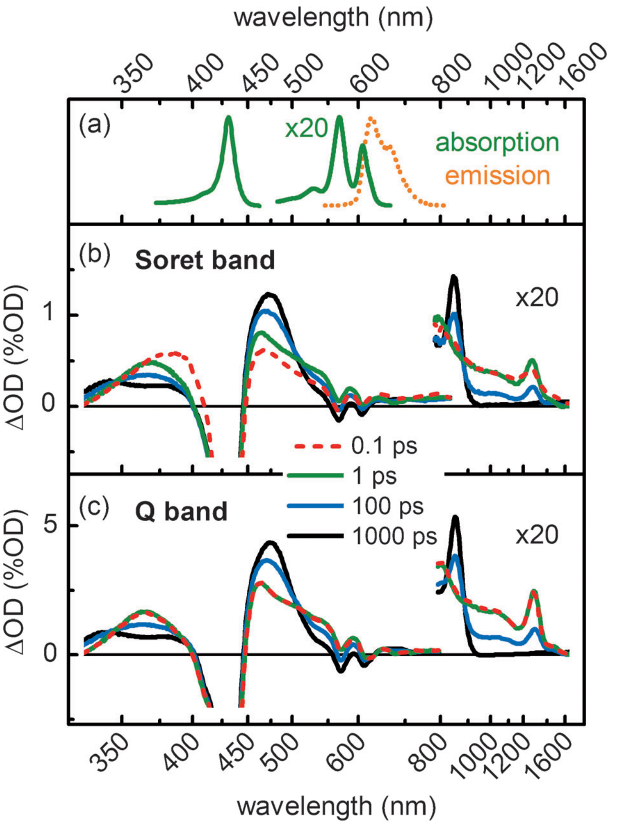

Figure 5. a) Absorption and emission spectra of CdTPP, (b) transient spectra after excitation of the Soret band at $\lambda = 425$ nm, and (c) transient spectra after excitation of the Q band at $\lambda = 620$ nm. For clarity, the 0.1 ps spectrum is indicated by a dashed line to signal that it is identical to the 1 ps spectrum after Q-band excitation within experimental precision and different for Soret-band excitation.

To confirm the existence of this E_g state, we first analyzed the spectral structure of the dynamics upon Q-band excitation of CdTPP. As explained above, the ESA spectrum of MgTPP upon probing the Q band was dominated by features caused by u to u transitions and the close similarity of the spectra taken from MgTPP and CdTPP indicate that the contributions from gerade states are minor. As in MgTPP, a strong band at $\lambda \approx 1280$ nm shows access of the $3E_u$ state and the peak at $\lambda \approx 1450$ nm indicates the Soret band. Because no state was found in the transient spectrum up to $\lambda = 1660$ nm, we performed single-color non-collinear optical parametric amplifier–optical parametric amplifier (NOPA-OPA) experiments with probe wavelengths up to $\lambda = 1750$ nm (see Figure 7). For probe wavelengths of $\lambda = 1280$ and 1500 nm, the recorded transients agree with the respective slices from our transient spectra. For $\lambda = 1660$ nm, the spectrum shows no signal and

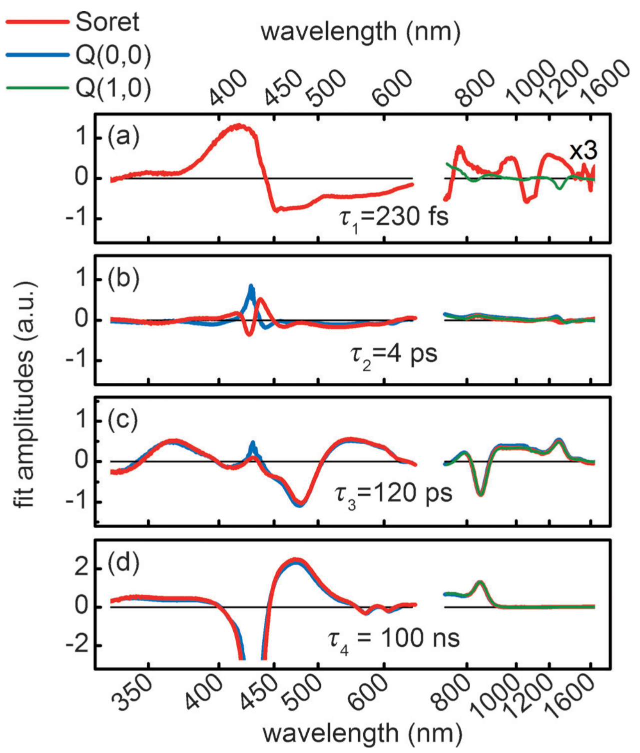

Figure 6. DADS for CdTPP upon excitation at the Q(0,0) (blue), Q(1,0) (green, only IR), and Soret (red) bands.

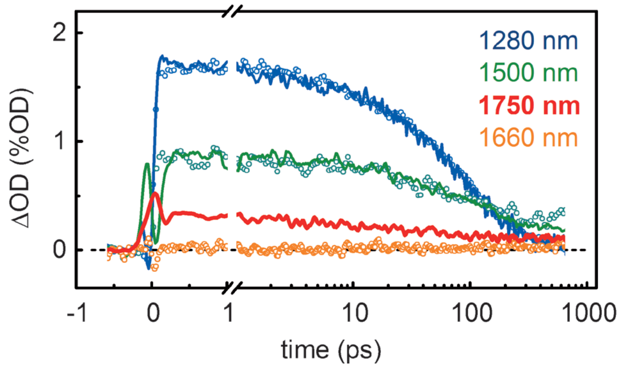

Figure 7. Single-color pump–probe experiments of CdTPP with a pump wavelength of $\lambda = 620$ nm and selected probe wavelengths. The open circles represent data taken from the transient spectrum with probe wavelengths of $\lambda = 1280$, 1550, and 1660 nm. The solid lines show NOPA-OPA measurements with probe wavelengths at $\lambda = 1280$, 1500, and 1750 nm.

we see an increased signal at $\lambda = 1750$ nm, which can be assigned to a rising band. Owing to missing alternatives, this band must be assigned to the dark $1E_g$ state, especially when comparing it to the distinctively weaker signal in MgTPP. The total energy of this state then results to about (2.75 ± 0.1) eV. Its small oscillator strength might be taken as an indication that the gerade states do not possess high oscillator strengths, even for [1+1] excitation. As a final result, we state that the triplet splitting in CdTPP is 1.47 eV ($\lambda = 846$ nm), as shown by the DADS in Figure 6 and the complete transient spectra in Figure S4 in the Supporting Information.

Conclusion

We performed pump–probe investigations of the Soret and Q bands of MgTPP and CdTPP in THF to decipher the dependence of the relaxation pathways and the excited-state manifolds from the central metal ion for closed d-shell atoms. The relaxation dynamics were monitored by measuring transient absorption spectra in the visible and NIR spectral regimes and the results were backed by ab initio calculations. Upon Soret excitation, the dynamics of CdTPP were significantly faster than for the other complexes, which depended on a dark E_g state. This state was located at the central N_4 cage and mediated the transition between the Soret and Q bands and took place with $(100 \pm 2)\%$ quantum yield. In MgTPP and ZnTPP the E_g state was higher in energy. This caused the internal conversion in CdTPP an order of magnitude faster than that in MgTPP for which relaxation required 3.2 ps. In summary, the light-induced reaction dynamics of porphyrins all proceeded along the same pathway and the only major modification between the different central metal ions were the lifetimes of the singlet and triplet states caused by the dark E_g state and different spin-orbit couplings.

Further investigations into different porphyrins include transition-metal atoms with open d shells and the dependence of the dynamics of the porphyrin cage.

Experimental Section

Sample preparation

5,10,15,20-Tetraphenylporphyrinato magnesium(II): The purified free-base *meso*-tetraphenylporphyrin was magnesiated by using the method optimized by Lindsey and Woodford[53] with a tenfold excess of magnesium dibromide diethyl etherate (413 mg, 1.62 mmol) in dry dichloromethane (8 mL) in the presence of triethylamine (0.45 mL) under an argon atmosphere. UV/Vis spectroscopy showed that metalation was completed within 15 min at room temperature. The reaction mixture was diluted with dichloromethane (25 mL) and washed twice (2×25 mL) with an aqueous solution of sodium hydrogen carbonate and then with distilled water. Column chromatography on neutral alumina eluted with dichloromethane containing 0.1 % triethylamine afforded the magnesium–triethylamine adduct (65 mg). A second chromatography step on alumina, which was eluted with pure dichloromethane freshly distilled from calcium hydride, gave—after evaporation of the solvent—a plum-colored powder, which was sublimed in vacuum (10^{-3} mbar) by heating to over 180 °C.

5,10,15,20-Tetraphenylporphyrinato cadmium(II): A solution of 5,10,15,20-tetraphenyl-porphyrin free of the corresponding chlorin (0.1 g, 0.16 mmol) in anhydrous DMF (10 mL) was degassed under nitrogen. Cadmium acetate monohydrate (Aldrich) was dehydrated by heating at 110 °C for 5 h under vacuum (<1 mbar). The anhydrous cadmium acetate (0.375 g, 1.6 mmol) was added to the violet solution of the porphyrin and heated at 120 °C for 1 h under an argon atmosphere. The solution changed color to pine green. The reaction mixture was extracted into dichloromethane (50 mL) and washed with water (2×50 mL). The organic layer was evaporated to afford, after drying overnight in vacuum, lavender–green crystals CdTPP (0.1 g, 87.5 %).

MgTPP and CdTPP were checked for impurities by ^{1}H NMR and UV/Vis absorption spectroscopy. The CdTPP spectra in anhydrous toluene and THF showed only a very small bathochromic shift of the two Q bands from $\lambda=568$ to 573 nm and from $\lambda=609$ to 615 nm, respectively, which we assigned to a solvatochromic effect (see Figure S5). For MgTPP, especially in THF, five-coordinated species should be prevalent, in addition to the six-coordinated one.[13] A four-coordinated Mg species within porphyrins and (bacterio)-chlorophylls has never been encountered experimentally in crystal structures owing to them being unstable and coordinatively unsaturated. Either solvent or even adventitious water molecules are spontaneously tightly bound, whereas in a protein environment, various polar amino acid residues function as apical ligands to the Mg atom.[9] However, upon vertical excitation with a rather large laser pulse width, the excited species are assumed to be of D_{4h} symmetry. Future experimental and theoretical studies will address this issue.

Experimental methods

Steady-state absorption spectra of MgTPP and CdTPP in THF were recorded by using a Varian Cary5E spectrophotometer and fluorescence spectra were recorded by using a Cary Eclipse fluorescence spectrophotometer.

For UV to visible and IR time-resolved pump–probe spectroscopy, we used a commercial 1 kHz Ti:sapphire-based laser system (CPA 2001; Clark-MXR), which generated pulses with a center wavelength of $\lambda=778$ nm, a full-width at half maximum (FWHM) of 170 fs pulses, and an output energy of 1 mJ. The pump was generated in a two-stage NOPA system and subsequently compressed with a pair of fused silica prisms down to 20 fs, which corresponded to a time–bandwidth product of 0.84. The excitation wavelength for both MgTPP and CdTPP was $\lambda=620$ nm. The spectral width was 35 nm. To ensure the same properties for the probe pulse during the experiment, we delayed the pump pulse with a commercial translation stage (M-531.PD; Physik Instrumente Inc.) and checked that the spatial overlap and size of the pump stayed constant when moving the delay stage.

For the UV and visible probe light, we generated a continuum in a moving 5 mm CaF_2 plate with the pump laser. A thin filter was used to block the region around the pump wavelength. To generate an IR probe continuum, we used the idler of a white-light-seeded $\lambda=778$ nm pumped collinear OPA centered at 2.1 μm. Focusing this idler onto a YVO_4 crystal allowed the generation of a continuum down to $\lambda=550$ nm.[54] The broadened 2.1 μm pump was cut off with a dielectric filter with an edge at $\lambda=1650$ nm.

For both continua, pump and probe were focused onto the sample under a small external angle of 4°. To minimize anisotropy effects, the polarization of the pump pulse was set at a magic angle with respect to the probe pulse by using an achromatic $\lambda/2$ wave plate. An additional polarizer after the sample minimized pump stray light. The probe beam was completely located within the excitation area of the pump pulse in the sample and its diameter was half of the pump beam ($1/e^2$ radius for intensity of pump $=w_0=135$ μm). The probe beam was spectrally dispersed and imaged onto a line array. For the UV to visible continuum, we used a fused silica prism to disperse the colors and imaged it onto a photodiode array (NMOS; S3902-512Q; Hamamatsu Inc.). The IR white light was dispersed with a SF10 prism and then focused on an InGaAs array. This allowed stepwise probing from $\lambda=290$ to 1660 nm. More details on the basic setup are given in Ref. [51] and the infrared extension will be discussed in a forthcoming publication.[55] Additionally NOPA-OPA measurements with $\lambda=620$ nm pumping and probing at $\lambda=1280$, 1550, and 1750 nm were performed. Therefore, we directly used the light from the collinear IR OPA as the probe light without any further IR continuum generation.

MgTPP and CdTPP were measured in a 1 mm cuvette from Hellma, as well as in a flowthrough cell. The optical density for MgTPP was 0.2, the pump energy was 800 nJ, and the pump intensity was 6.0×10^{10} W cm^{-2}. For CdTPP, the optical density was 0.3, the pump energy was 200 nJ, and the pump intensity was 2.0×10^{10} W cm^{-2}. All experiments were performed at room temperature.

Acknowledgements

This study was funded by the Deutsche Forschungsgemeinschaft (DFG), the State Baden-Württemberg and the Karlsruhe Institute of Technology (KIT) through the Center for Functional Nanostructures (CFN, projects C3.2 and C3.5). O.S. is thankful for financial support from the Humboldt-Foundation and the Wenner-Gren Foundation. M.B., O.S., and E.R. are furthermore grateful to be supported by the DFG Cluster of Excellence: Munich Centre for Advanced Photonics.

Keywords: dark states · density functional calculations · femtosecond spectroscopy · porphyrinoids

[1] a) H. Shinmori, T. Kajiwara, A. Osuka, *Tetrahedron Lett.* **2001**, *42*, 3617; b) A. Kay, R. Humphry, M. Grätzel, *J. Phys. Chem.* **1994**, *98*, 952; c) D. Wu, Z. Shen, Z. Xue, M. You, *Chin. J. Inorg. Chem.* **2007**, *23*, 1.

[2] a) E. D. Sternberg, D. Dolphin, C. Brückner, *Tetrahedron* **1998**, *54*, 4151; b) X. Chen, C. M. Drain, *Drug Des. Rev.–Online* **2004**, *1*, 215; c) M. P. Donzello, C. Ercolani, P. A. M. P. Stuzhin, *Coord. Chem. Rev.* **2006**, *250*, 1530; d) V. Gottumukkala, R. J. Luguya, F. R. Fronczeck, M. G. H. Vincente, *Bioorg. Med. Chem.* **2005**, *13*, 1633.

[3] a) C. A. Mirkin, M. A. Ratner, *Annu. Rev. Phys. Chem.* **1992**, *43*, 719; b) M. J. Gunter, M. R. Johnston, *J. Chem. Soc. Chem. Commun.* **1992**, 1163; c) K. Sienicki in *Molecular Electronics and Molecular Electronic Devices, Vol. 3*, CRC Press, Boca Raton, **1994**.

[4] J. Karolczak, D. Kowalska, A. Lukaszewicz, A. Maciejewski, R. P. Steer, *J. Phys. Chem. A* **2004**, *108*, 4570.

[5] H. Z. Yu, J. S. Baskin, B. Steiger, C. Z. Wan, F. C. Anson, A. H. Zewail, *Chem. Phys. Lett.* **1998**, *293*, 1.

[6] R. E. Haddad, S. Gazeau, J. Pécaut, J.-C. Marchon, C. J. Medforth, J. A. Shelnutt, *J. Am. Chem. Soc.* **2003**, *125*, 1253.

[7] A. Marcelli, P. Foggi, L. Moroni, C. Gellini, P. R. Salvi, *J. Phys. Chem. A* **2008**, *112*, 1864.

[8] a) L. Luo, C.-H. Chang, Y.-C. Chen, T.-K. Wu, E. W.-G. Diau, *J. Phys. Chem. B* **2007**, *111*, 7656; b) A. Gadalla, J.-B. Beaufrand, M. Bowen, S. Boukari, E. Beaurepaire, O. Crégut, M. Gallart, B. Hönerlage, P. Gilliot, *J. Phys. Chem. C* **2010**, *114*, 17854; c) R. Kumble, S. Palese, V. S.-Y. Lin, M. J. Therien, R. M. Hochstrasser, *J. Am. Chem. Soc.* **1998**, *120*, 11489.

[9] T. S. Balaban, P. Braun, C. Hättig, A. Hellweg, J. Kem, W. Saenger, A. Zouni, *Biochim. Biophys. Acta Bioenergetics* **2009**, *1787*, 1254.

[10] A. Hazell, *Acta. Crystallogr. Sect. C* **1986**, *42*, 296.

[11] A. Hazell, *Acta. Crystallogr. Sect. C* **1984**, *40*, 751.

[12] J. L. Hoard in *Porphyrins and Metalloporphyrins* (Eds.: K. M. Smith), Elsevier, Amsterdam, **1975**, pp. 317.

[13] O. Schalk, Y. Liang, A.-N. Unterreiner, *Z. Phys. Chem. (Muenchen Ger.)* **2013**, *227*, 35.

[14] M. Gouterman in *The Porphyrins, Vol. 3* (Eds.: D. H. Dolpin), Academic Press, New York, **1978**, pp. 1.

[15] K. Kalyanasundaram, *Photochemistry of Polypyridine and Porphyrin Complexes*, Academic Press, London, **1992**.

[16] V. V. Apanasovich, E. G. Novikov, N. N. Yatskov, R. B. M. Koehorst, T. J. Schaafsma, A. van Hoek, *J. Appl. Spectrosc.* **1999**, *66*, 613.
[17] S. F. Shkirman, K. N. Solov'ev, T. F. Kachura, S. A. Arabei, E. D. Skakovskii, *J. Appl. Spectrosc.* **1999**, *66*, 68.
[18] I. T. Oliver, W. A. Rawlinson, *Biochem. J.* **1955**, *61*, 641.
[19] L. Edwards, D. H. Dolpin, M. Gouterman, *J. Mol. Spectrosc.* **1971**, *38*, 16.
[20] L. Edwards, D. H. Dolpin, M. Gouterman, *J. Mol. Spectrosc.* **1970**, *35*, 90.
[21] M. Gouterman, *J. Chem. Phys.* **1959**, *30*, 1139.
[22] M. Gouterman, *J. Mol. Spectrosc.* **1961**, *6*, 138.
[23] C. Weiss, H. Kobayashi, M. Gouterman, *J. Mol. Spectrosc.* **1965**, *16*, 415.
[24] E. J. Baerends, G. Ricciardi, A. Rosa, S. J. A. van Gisbergen, *Coord. Chem. Rev.* **2002**, *230*, 5.
[25] H. Solheim, K. Ruud, S. Coriani, P. Norman, *J. Phys. Chem. A* **2008**, *112*, 9615.
[26] G. A. Peralta, M. Seth, T. Ziegler, *Inorg. Chem.* **2007**, *46*, 9111.
[27] H. Chosrowjan, S. Tanigichi, T. Okada, S. Takagi, K. Tokumaru, *Chem. Phys. Lett.* **1995**, *242*, 644.
[28] G. G. Gurzadyan, T.-H. Tran-Thi, T. Gustavsson, *J. Chem. Phys.* **1998**, *108*, 385.
[29] H. Z. Yu, J. S. Baskin, A. H. Zewail, *J. Phys. Chem. A* **2002**, *106*, 9845.
[30] U. Tripathy, D. Kowalska, X. Liu, S. Velate, R. P. Steer, *J. Phys. Chem. A* **2008**, *112*, 5824.
[31] X. Liu, U. Tripathy, S. V. Bhosale, S. J. Langford, R. P. Steer, *J. Phys. Chem. A* **2008**, *112*, 8986.
[32] S. Sorgues, L. Poisson, K. Raffael, L. Krim, B. Soep, N. Shafizadeh, *J. Chem. Phys.* **2006**, *124*, 114302.
[33] N. Mataga, Y. Shibata, H. Chosrowjan, N. Yoshida, A. Osuka, *J. Phys. Chem. B* **2000**, *104*, 4001.
[34] M. Kullmann, A. Hipke, P. Nuernberger, T. Bruhn, D. C. G. Götz, M. Sekita, D. M. Guldi, G. Bringmann, T. Brixner, *Phys. Chem. Chem. Phys.* **2012**, *14*, 8038.
[35] A. Lukaszewicz, J. Karolczak, D. Kowalska, A. Maciejewski, M. Ziolek, R. P. Steer, *Chem. Phys.* **2007**, *331*, 359.
[36] S. Velate, X. Liu, R. P. Steer, *Chem. Phys. Lett.* **2006**, *427*, 295.
[37] J. S. Baskin, H. Z. Yu, A. H. Zewail, *J. Phys. Chem. A* **2002**, *106*, 9837.
[38] X. Liu, E. K. L. Yeow, S. Velate, R. P. Steer, *Phys. Chem. Chem. Phys.* **2006**, *8*, 1298.
[39] G. Niranjian, V. Marat, J. Lasse, K. Karol, *J. Phys. Chem. A* **2009**, *113*, 6041.
[40] Z.-L. Cai, M. J. Crossley, J. R. Reimers, R. Kobayashi, R. D. Amos, *J. Phys. Chem. B* **2006**, *110*, 15624.
[41] R. Kobayashi, R. D. Amos, *Chem. Phys. Lett.* **2006**, *420*, 106.
[42] O. Schalk, H. Brands, T. S. Balaban, A.-N. Unterreiner, *J. Phys. Chem. A* **2008**, *112*, 1719.
[43] D. B. Moravec, B. M. Lovaasen, M. D. Hopkins, *J. Photochem. Photobiol. A* **2013**, *254*, 20.
[44] M. Gouterman, F. P. Schwarz, P. D. Smith, *J. Chem. Phys.* **1973**, *59*, 676.
[45] A. Harriman, *J. Chem. Soc. Faraday Trans. 2* **1981**, *77*, 1281.
[46] M. W. Schmidt, K. K. Baldridge, J. A. Boatz, S. T. Elbert, M. S. Gordon, J. H. Jensen, S. Koseki, N. Matsunaga, K. A. Nguyen, S. J. Su, T. L. Windus, M. Duquis, J. A. Montgomery, *J. Comput. Chem.* **1993**, *14*, 1347.
[47] M. S. Gordon, M. W. Schmidt in *Theory and Applications of Computational Chemistry, the First Forty Years* (Eds.: C. E. Dykstra, G. Frenking, K. S. Kim, G. E. Scuseria), Elsevier, Amsterdam **2005**, pp. 1167.
[48] D. Sundholm, *Chem. Phys. Lett.* **2000**, *317*, 392.
[49] R. D. Shannon, C. T. Prewitt, *Acta Crystallogr. Sect. B* **1969**, *25*, 925.
[50] U. Even, J. Magen, J. Jortner, J. Friedman, H. Levaon, *J. Chem. Phys.* **1982**, *77*, 4374.
[51] U. Megerle, I. Pugliesi, C. Schriever, C. F. Sailer, E. Riedle, *Appl. Phys. B* **2009**, *96*, 215.
[52] D. Sundholm, *Phys. Chem. Chem. Phys.* **2000**, *2*, 2275.
[53] J. S. Lindsey, J. N. Woodford, *Inorg. Chem.* **1995**, *34*, 1063.
[54] M. Bradler, P. Baum, E. Riedle, *Appl. Phys. B* **2009**, *97*, 561.
[55] E. Riedle, M. Bradler, M. Wenninger, C. F. Sailer, I. Pugliesi. *Faraday Disc.*, **2013**, DOI: 10.1039/C3FD00010A.

Received: April 19, 2013